FULL PAPER

Dalton
www.rsc.org/dalton

Interaction of macrocyclic copper(II) complexes with calf thymus DNA: effects of the side chains of the ligands on the DNA-binding behaviors

Jie Liu,[a,b] Hao Zhang,[c] Caihong Chen,[a] Hong Deng,[a] Tongbu Lu[a] and Liangnian Ji*[a]

[a] *The Key Laboratory of Gene Engineering of Ministry of Education, School of Chemistry and Chemical Engineering, Zhongshan University, Guangzhou 510275, P. R. China. E-mail: cesjln@zsu.edu.cn*

[b] *Department of Chemistry and Chemical Engineering, Zhengzhou Institute of Technology, Zhengzhou 450052, P. R. China*

[c] *Department of Chemistry, The Hong Kong University of Science and Technology, Clear Water Bay, Kowloon, Hong Kong*

Received 24th June 2002, Accepted 24th October 2002
First published as an Advance Article on the web 27th November 2002

Three macrocyclic copper(II) complexes of formula $CuL^1(ClO_4)_2$ (L^1 = 1,4,8,11-tetraazacyclotetradecane), CuL^2Cl_2 (L^2 = 3,10-bis-phenethyl-1,3,5,8,10,12-hexaazacyclotetradecane) and CuL^3Cl_2 (L^3 = 3,10-bis-*n*-propyl-1,3,5,8,10,12-hexaazacyclotetradecane) have been synthesized and characterized by elemental analysis, infrared spectroscopy and mass spectrometry. X-Ray structural analysis of $CuL^2(ClO_4)_2$ showed each copper atom to be coordinated to four nitrogen atoms in the macrocycle, which has a square-planar coordination geometry. Absorption and fluorescence spectral studies, circular dichroic spectral and viscometric studies have been carried out to assess the interaction of the three complexes with calf thymus DNA. The results suggest that three complexes can bind to DNA by different binding modes. $[CuL^1]^{2+}$ and $[CuL^3]^{2+}$ can bind to DNA by electrostatic interaction whereas $[CuL^2]^{2+}$ may bind to DNA by intercalation of the aromatic ring into the base pairs of DNA. The functional groups on the side chain of the macrocycle play a key role in deciding the mode and extent of binding of the copper complexes to DNA. The copper complexes exhibit nuclease activities, in which circular plasmid pUC18 DNA is initially converted to nicked DNA.

Introduction

The increasing interest in using macrocycles and their coordination compounds as artificial restriction enzymes for cleaving DNA and RNA has prompted us to investigate the application of macrocyclic transition metal complexes in this area. The specific recognition and oxidative cleavage of DNA by macrocyclic nickel(II) complexes with a square-planar structure has been well documented,[1–8] but the binding mode and cleavage mechanism still has not been fully verified.

Copper is a bio-essential element and copper complexes have been extensively utilized in metal-mediated DNA cleavage for the generation of activated oxygen species.[9] It has been reported that tetraaza macrocyclic copper coordination compounds have anti-HIV activities.[10] However, only a few attempts have been made to understand the binding studies of macrocyclic copper(II) complexes with DNA.[11–14] Studies have shown that these macrocyclic complexes can react with DNA in different binding fashions and exhibit effective nuclease activities. Therefore, extensive studies using different structural macrocycles to evaluate and understand the factors that determine the mode and mechanism of the binding interaction of macrocyclic transition metal complexes with DNA are necessary. So we recently investigated the effect of size and substitutional groups of a variety of macrocyclic polyamine ligands and their copper complexes on the nature of DNA binding with macrocyclic copper(II) complexes.[15–16]

Here, we describe the synthesis and characterization of three complexes: $CuL^1(ClO_4)_2$ (L^1 = 1,4,8,11-tetraazacyclotetradecane), CuL^2Cl_2 (L^2 = 3,10-bis-phenethyl-1,3,5,8,10,12-hexaazacyclotetradecane) and CuL^3Cl_2 (L^3 = 3,10-bis-*n*-propyl-1,3,5,8,10,12-hexaazacyclotetradecane) (see Scheme 1). Their interaction with calf thymus DNA (CT DNA) was investigated by electronic absorption, circular dichroism, fluorescence spectroscopy and viscosity measurements. The three ternary copper(II) complexes are symmetrical derivatives of tetraazacyclotetradecane, which possess different side chains at 3,10-position. Their different structural features on the side chains may result in different DNA binding interactions by intercalation, hydrogen bonding, van der Waals forces, hydrophobic interaction or coordination between the cupric ion in the complex and the base nitrogen in DNA. Such a ligand modification would provide an opportunity to obtain structural insight into the binding event. Our aim is to understand the selectivity and efficiency of DNA recognized and cleaved by

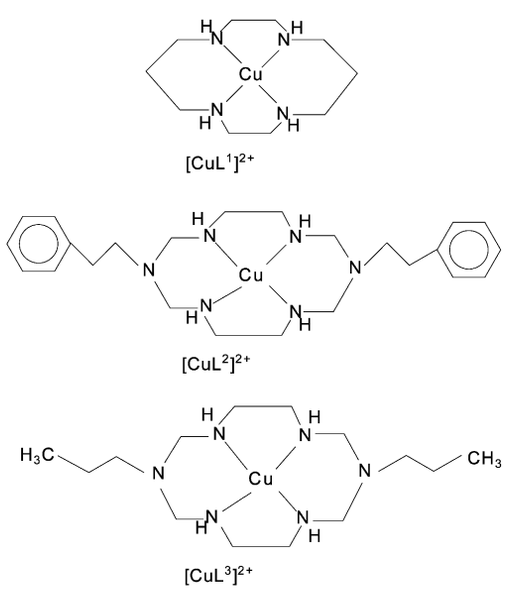

Scheme 1 Chemical structures of the macrocyclic copper(II) complexes

DOI: 10.1039/b206079p

different structural macrocyclic copper complexes, and to develop new effective cleaving agents or useful DNA probes.

Experimental

Materials and methods

All materials and solvents were purchased commercially and used without further purification unless otherwise noted. Solutions of CT DNA in 50 mM NaCl/5 mM Tris-HCl (pH = 7.0) gave a ratio of UV absorbance at 260 and 280 nm, A_{260}/A_{280}, of *ca.* 1.8–1.9, indicating that the DNA was sufficiently free of protein.[17] Concentrated stock solution of DNA was prepared in 5 mM Tris-HCl/50 mM NaCl in water, pH = 7.0, and the concentration of DNA was determined by UV absorbance at 260 nm after 1:100 dilutions. The molar absorption coefficient was taken as 6600 M^{-1} cm^{-1}.[18] Stock solutions were stored at 4 °C and were used after no more than four days. Doubly distilled water was used to prepare buffer solutions.

Physical measurements

Carbon, hydrogen and nitrogen were determined using an Elementar Vario EL elemental analyser. UV-VIS spectra were recorded using a Shimadzu UV-3101PC spectrophotometer. Infrared spectra were recorded in the 4000–400 cm^{-1} region using KBr pellets and a Bruker EQUINOX 55 spectrometer and an RF-4500 spectrophotometer. Fast atomic bombardment mass spectra (FAB-MS) were obtained using a VG ZAB-HS spectrometer in a 3-nitrobenzyl alcohol matrix. The circular dichroism (CD) spectra were taken on a JASCO-J20C or a JASCO-J715 spectropolarimeter. Fluorescence determinations were performed using a Hitachi RF-4500 spectrophotometer.

Viscosity experiments were carried on an Ubbelodhe viscometer, immersed in a thermostated water-bath maintained at 30 ± 0.1 °C. DNA samples of approximately 0.5 mM were prepared by sonicating in order to minimize complexities arising from DNA flexibility.[19] Flow time was measured with a digital stopwatch, and each sample was measured three times and an average flow time was calculated. Data were presented as $(\eta/\eta_0)^{1/3}$ *versus* the concentration of the macrocyclic copper(II) complex, where η is the viscosity of DNA in the presence of the complex, and η_0 is the viscosity of DNA alone. Viscosity values were calculated from the observed flow time of DNA-containing solutions ($t > 100$ s) corrected for the flow time of the buffer alone (t_0): $\eta = t - t_0/t_0$.[20]

The gel electrophoresis experiments were performed by incubation at 35 °C for 1.5 h as follows: pUC18 DNA 30 μM, 50 μM copper complex, 500 μM H_2O_2 and/or 500 μM 2-mercaptoethanol in 50 mM Tris-HCl/18 mM NaCl buffer (pH = 7.2). The samples were subjected to electrophoresis for 4 h at 40 V on a 1% agarose gel using a Tris-boric acid–EDTA buffer, pH = 8.3. After electrophoresis, the gel was stained using 1 μg cm^{-3} ethidium bromide and photographed under UV light.

Synthesis

$CuL^1(ClO_4)_2$ (1). A mixture of 1,4,8,11-tetraazacyclotetradecane (0.1 g, 0.5 mmol) and $Cu(ClO_4)_2 \cdot 6H_2O$ (0.185 g, 0.5 mmol) was stirred in methanol solution (15 mL) for 4 h. The violet-red solution was filtered, and the filtrate was allowed to stand at room temperature. Several days later, the violet-red crystals formed were washed with methanol/diethyl ether and further dried *in vacuo*. Yield: 70%. (Found: C, 25.87; H, 5.224; N, 12.07. Calc. for $CuC_{10}H_{24}N_4Cl_2O_8$: C, 25.95; H, 5.227; N, 12.11%.) IR (KBr, ν/cm^{-1}): 3210(s), 2943(m), 2864(m). FAB-MS: *m*/*z* 360 [M − ClO_4 − $3H^+$], 263 [M − $2ClO_4$].

$CuL^2Cl_2 \cdot 2H_2O$ (2). To a stirred methanol solution (10 mL) of $CuCl_2 \cdot 6H_2O$ (1.7 g, 0.01 mol) was slowly added ethylenediamine (1.4 g, 0.02 mol), formaldehyde (4.0 mL) and phenethylamine (2.9 g, 0.024 mol). The mixture was heated under reflux for 24 h. The solution was filtered hot, and the filtrate was allowed to stand at room temperature. The purple precipitate formed was filtered off, washed with methanol and further dried *in vacuo*. Yield: 32%. (Found: C, 49.86; H, 7.306; N, 14.74. Calc. for $CuC_{24}H_{42}N_6Cl_2O_2$: C, 49.64; H, 7.233; N, 14.68%.) IR (KBr, ν/cm^{-1}): 3485(s), 3246(m), 3179(m), 2936(m), 1602(m). FAB-MS: *m*/*z* 508 [M − Cl], 473 [M − 2Cl].

Crystalline $CuL^2(ClO_4)_2$ for X-ray crystallography was obtained by adding an excess amount of $NaClO_4$ to the solution of $[CuL^2]Cl_2$. The clear solution was allowed to stand at room temperature until violet-red crystals formed.

$CuL^3Cl_2 \cdot H_2O$ (3). This complex was obtained by a procedure similar to that described for (2) above except for the use of *n*-propylamine instead of phenethylamine. Yield: 57%. (Found: C, 36.80; H, 8.439; N, 17.82. Calc. for $CuC_{14}H_{38}N_6Cl_2O_2$: C, 36.80; H, 8.383; N, 18.40%.) IR (KBr, ν/cm^{-1}): 3741(s), 3212(m), 3182(m), 2962(m), 2874(m), 1603(w). FAB-MS: *m*/*z* 386 [M − Cl], 350 [M − 2Cl].

X-Ray crystallography

Violet-red crystals of $CuL^2(ClO_4)_2$ suitable for single-crystal X-ray diffraction with a size of 0.38 × 0.17 × 0.12 mm were selected. Data were collected with graphite-monochromated MoKα (λ = 0.71073 Å) radiation. The structure was solved by direct methods and refined with a full-matrix least-square technique using SHELXL-93 programes.[21] Crystal parameters and details of the data collection and refinement are given in Table 1.

CCDC reference number 177798.

See http://www.rsc.org/suppdata/dt/b2/b206079p/ for crystallographic data in CIF or other electronic format.

Table 1 Crystal data and structure refinement details for $CuL^2(ClO_4)_2$

Empirical formula	$C_{24}H_{34}Cl_2CuN_6O_8$
Formula weight	669.01
Temperature/K	293(2)
Wavelength/Å	0.71073
Crystal system, space group	Triclinic, $P\bar{1}$
a/Å	8.274(2)
b/Å	8.412(2)
c/Å	11.616(2)
α/°	85.51(3)
β/°	76.37(3)
γ/°	68.25(3)
V/Å^3	729.7(3)
Z, D_c/Mg m^{-3}	1, 1.522
Absorption coefficient/mm^{-1}	0.988
F(000)	347
Crystal size/mm	0.38 × 0.17 × 0.12
θ Range for data collection/°	*ca.* 14.71–21.96
Limiting indices	$-7 \le h \le 8$ $-8 \le k \le 8$ $-10 \le l \le 12$
Reflections collected/unique	1794/1234 (R_{int} = 0.0261)
Completeness to θ = 21.96° (%)	69.0
Max., min. transmission	0.8906, 0.7052
Goodness-of-fit on F^2	1.060
Final *R* indices [$I > 2\sigma(I)$]	$R1$ = 0.0576, $wR2$ = 0.1397
R indices (all data)	$R1$ = 0.0673, $wR2$ = 0.1460
Largest diff. peak and hole/e Å $^{-3}$	0.418 and −0.458
Data/restraints/parameters	1234/0/188

Results and discussion

Synthesis

Complex **1** was prepared using standard synthetic methods. Complexes **2** and **3** were obtained by template condensation reactions involving formaldehyde and amines as described in eqn. (1), where X = Py, CH_3.

Table 2 Selected bond lengths (Å) and angles (°) for $CuL^2(ClO_4)_2$

Cu(1)–N(2)#1	2.001(5)	Cu(1)–N(1)#1	2.017(5)
N(2)#1–Cu(1)–N(2)	180.0	N(2)#1–Cu(1)–N(1)#1	86.0(2)
N(2)–Cu(1)–N(1)#1	94.0(2)	C(1)–N(1)–Cu(1)	106.2(4)
C(4)#1–N(1)–Cu(1)	114.7(4)	C(2)–N(2)–C(3)	114.3(6)
C(2)–N(2)–Cu(1)	106.4(4)	C(3)–N(2)–Cu(1)	114.3(6)
C(5)–N(3)–C(3)	120.9(9)	C(5)–N(3)–C(4)	120.1(9)
C(3)–N(3)–C(4)	117.2(7)	N(1)–C(1)–C(2)	108.5(6)
N(2)–C(2)–C(1)	108.6(6)	N(3)–C(3)–N(2)	113.9(6)
N(3)–C(4)–N(1)#1	113.3(6)	C(6)–C(5)–N(3)	146(4)

Symmetry transformations used to generate equivalent atoms: #1 $-x$, $-y$, $-z$.

$$Cu^{2+} + NH_2CH_2CH_2NH_2 + CH_2O + NH_2\text{–}(CH_2)_2\text{–}X \rightarrow [CuL]^{2+} \quad (1)$$

The electronic absorption spectra for the aqueous solutions of $CuL^1(ClO_4)_2$, $CuL^2(ClO_4)_2$ and $CuL^3(ClO_4)_2$ show that d–d transitions of the complexes occur at 500–504 nm, which is the characteristic chromophore for the square-planar Cu(II) complex. In addition, these Cu(II) complexes show no spectral changes when they are converted to the form of CuL^1Cl_2, CuL^2Cl_2 and CuL^3Cl_2, respectively. This indicates that the Cu(II) ion in the complex forms the same square-planar geometry in water, in which the water molecules or Cl^- ions do not occupy the axial positions of the Cu(II) ion.

Crystal structure of $CuL^2(ClO_4)_2$

An ORTEP diagram of the cation of $CuL^2(ClO_4)_2$ with the atomic numbering scheme is shown in Fig. 1. Selected bond lengths and angles are given in Table 2.

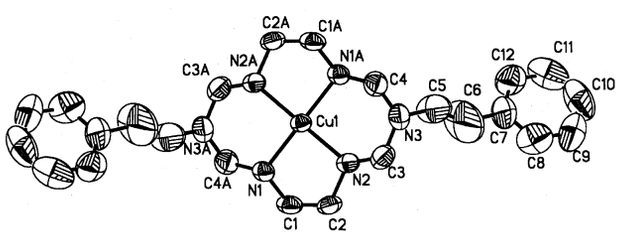

Fig. 1 ORTEP drawing of $CuL^2(ClO_4)_2$ and the atom numbering scheme.

The Cu(II) ion in the complex is coordinated by the four secondary nitrogen donors of the macrocycle and forms a square-planar geometry. The average Cu–N bond distance is 2.009 Å, which is close to *ca.* 2.0–2.2 Å of square-planar tetraaza macrocyclic copper(II) complexes.[22–23] The bond angle of N–Cu–N is 180.0°, and thus the nitrogen donors form a perfect plane including the Cu(II) ion. The bite angles of five- and six-membered chelate rings are 86.0(2) and 94.0(2)°, respectively. These are normally observed values for the bite distances and angles for the five-membered chelate rings in the square-planar Ni(II) complexes with a 14-membered macrocycle.[24] The macrocycle adopts an *R*,*R*,*S*,*S* configuration, which is the most thermodymatically stable form.

The aromatic rings on the side chain of the neighboring macrocycle are parallel, and their distances are 2.6032, 3.3542 Å, respectively. This suggests that the neighboring aromatic rings form a π–π stacking interaction.

Electronic absorption titration

Electronic absorption spectroscopy is often employed to ascertain the binding of complexes with DNA. A complex bound to DNA through intercalation is characteristic of hypochromism and red shift, due to the intercalative mode involving a strong stacking interaction between an aromatic chromophore and the base pairs of DNA. The extent of the hypochromism is commonly consistent with the strength of intercalative interaction.[3,25–26]

Table 3 Effects of CT DNA on the absorbance bands and binding constants of **1**, **2** and **3**

	λ_{max}/nm				
Compound	Free	Bound	$\Delta\lambda$/nm	H[a](%)	K_b/M^{-1}
1	253.4	254.1	0.7	+3.9	1.3×10^2
2	252.4	252.4	0	−17.6	2.1×10^4
	237.6	237.4	−0.2	−15.0	
	195.8	204.5	8.7	−9.0	
3	250.6	252.6	2.0	+11.6	4.6×10^2
	231.6	231.6	0	+0.1	

[a] +, hyperchromism; −, hypochromism.

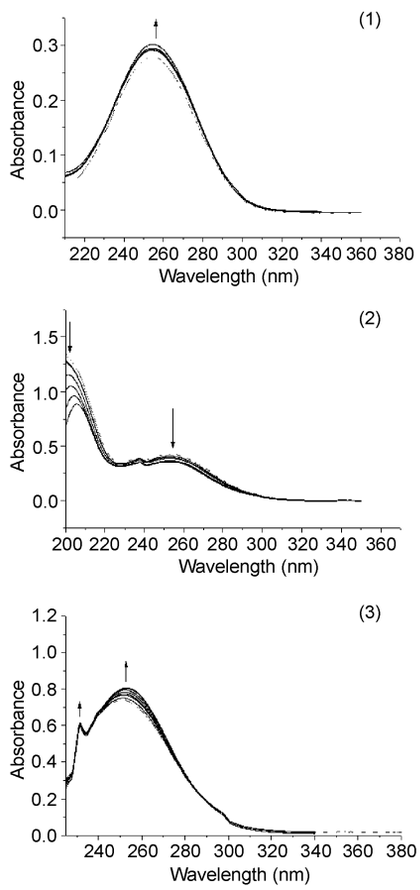

Fig. 2 Absorption spectra of **1**, **2** and **3** in the absence (---) and presence (—) of increasing amounts of DNA. [CuL] = 40 μM. Arrows show the absorbance changes upon increasing DNA concentration.

The absorption spectra of the three complexes in the absence and the presence of calf thymus DNA are showed in Fig. 2. In the UV region, all of the present macrocyclic copper(II) complexes exhibit an intense absorption band around 250 nm which is attributed to an n⟶π* or π⟶π* transition absorption. With increasing concentration of calf thymus DNA, the absorption bands of the complexes are affected, resulting in the obvious tendency of hyperchromism or hypochromism and a slight red shift. An electronic interaction between the copper(II) coordination compounds and DNA can be observed through the data of hyperchromism or hypochromism and shifts in the absorbance maxima of the copper(II) complexes (Table 3).

The copper(II) complexes can bind to the double-stranded DNA in different binding modes on the basis of their structure

and charge, and type of ligands. The hypochromism of *ca.* 17.6% for the band of 252 nm for **2** suggests that the complex binds to DNA strongly. The absorption band at 196 nm exhibits hypochromism about 9%, and bathochromism of about 9 nm. The observed considerable hypochromism and bathochromism for **2** are large compared to that observed for potential intercalators.[18,27] Structurally, the ligand of **2** should provide an aromatic moiety extending from the side chain through which to overlap with the stacking base pairs of the DNA helix by intercalation. It has been reported that a square-planar copper(II) *meso*-tetra(*N*-methyl-4-pyridyl)porphyrin, analogous to **2**, containing four positively charged pyridyl rings, binds to DNA *via* normal intercalation.[28] However, the five-coordinated copper(II) complex, $Cu(IDB)Cl_2$ (IDB = 1,5-bis(2-benzimidazolyl)diethylamine), with the aromatic moiety extending from the metal center does not bind to DNA by insertion; instead, the DNA base nitrogen atoms substitute for the two Cl^- ions and then coordinate to the cupric ion in the complex.[9] So these observations led us to suspect that complex **2** may bind to DNA by insertion of the aromatic ring between adjacent base pairs on the DNA duplex. But this needs further clarification of the DNA-binding mode of the complex by viscosity measurements.

Since complexes **1** and **3** do not contain any fused aromatic ring to facilitate intercalation, classical intercalative interaction would be impossible. The hyperchromism of complexes **1** and **3** caused by addition of CT DNA imply that the binding modes of the two complexes with DNA are different from that exhibited by **2**. Similar hyperchromism has been observed for the Soret bands of certain porphyrins when interacted with DNA but has not yet been clearly explained.[29] The complex $Cu(HTCD)^{2+}$ (HTCD = 2,2,9,9-tetramethyl-4,11-dimethyl-1,5,8,12-tetraazacyclotetradecane) analogous to complexes **1** and **3** but containing six methyl groups on the macrocycle, binds to DNA by van der Waals interactions between the methylene groups and the thymine methyl group, and hydrophobic interactions between the methyl groups in the complex and the DNA interior.[9] DNA possesses several hydrogen bonding sites which are accessible both in the minor and major grooves, while the two complexes contain four coordinated amine –NH– groups in the macrocycle which could form hydrogen bonding with the base pairs in DNA.

For the three copper complexes, the binding constants, K_b, have been determined from the spectroscopic titration data using the equation:[30]

$$[DNA]/(\varepsilon_a - \varepsilon_f) = [DNA]/(\varepsilon_b - \varepsilon_f) + 1/K_b(\varepsilon_a - \varepsilon_f)$$

where ε_a, ε_f and ε_b correspond to $A_{obs.}$/[Cu], the extinction coefficient of the free copper complex, and the extinction coefficient for the copper complex in the fully bound form, respectively. A plot of $[DNA]/(\varepsilon_a - \varepsilon_f)$ *vs.* [DNA] will have a slope of $1/(\varepsilon_b - \varepsilon_f)$ and an intercept equal to $1/K_b(\varepsilon_b - \varepsilon_f)$. K_b is then given by the ratio of the slope to the intercept.

The binding constants obtained for the complexes **1**, **2** and **3** are 1.3×10^2, 2.1×10^4, and 4.6×10^2 M^{-1}, respectively. The K_b value for **2** is higher than those for **1** and **3**, but their K_b values are lower than those observed for typical classical intercalators (ethidium–DNA, 1.4×10^6 M^{-1}, in 25 mM Tris-HCl/40 mM NaCl buffer, pH = 7.9[31]). This is indicative of the binding of the complexes with DNA with an affinity less than the classical intercalators.

Fluorescence spectroscopic studies

Ethidium bromide (EB) emits intense fluorescence in the presence of DNA due to its strong intercalation between the adjacent DNA base pairs. It was previously reported that the enhanced fluorescence can be quenched by the addition of a second molecule.[32] Two mechanisms have been proposed to account for the quenching: the replacement of molecular fluorophores, and/or electron transfer.[32–33] The quenching extent of the fluorescence of EB bound to DNA is utilized to determine the extent of binding between the second molecule and DNA.

The emission spectra of EB bound to DNA in the absence and presence of the copper complexes are given in Fig. 3. The

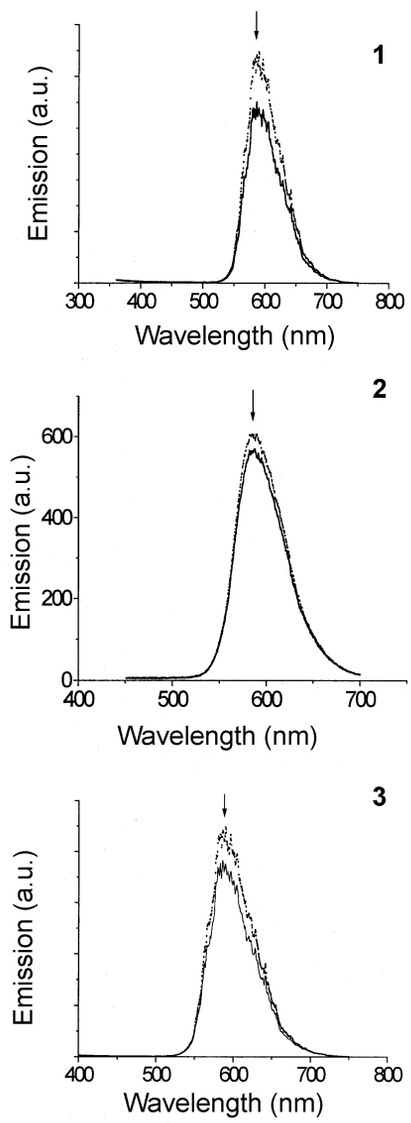

Fig. 3 Emission spectra of EB bound to DNA in the absence (- - -) and presence (—) of **1**, **2** and **3**. [CuL] = 1 mM, [CuL]/[DNA] = 0, 0.2, 0.4, 0.6, 0.8; λ_{ex} = 310 nm.

addition of the complexes to DNA pretreated with ethidium bromide causes a reduction in the emission intensity, indicating the competition with EB in binding to DNA. Liu *et al.*[12] found that the fluorescence quenching of EB–DNA by the tetraaza macrocyclic complexes may be due to the replacement of the DNA intercalator, *i.e.* EB. This means that the complexes interact with the same sites as EB does. The structure of complex **1** is analogous to the tetraaza macrocyclic complexes. The results illustrate that the three macrocyclic copper complexes can more or less quench the fluorescence of the EB–DNA complex. Complex **2** would be expected to produce a large reduction in emission intensity in the presence of DNA; however, a slight reduction is observed. This is may be due to the longer side chain which hinders intercalation of the ligand into DNA, and it is implied that the DNA-binding of **2** is expected to occur by weak insertion.

Circular dichroism

The CD spectrum of CT DNA exhibits a positive band at 275 nm due to base stacking and a negative band at 245 nm due to the helicity of DNA (Fig. 4). Incubation of the DNA with the

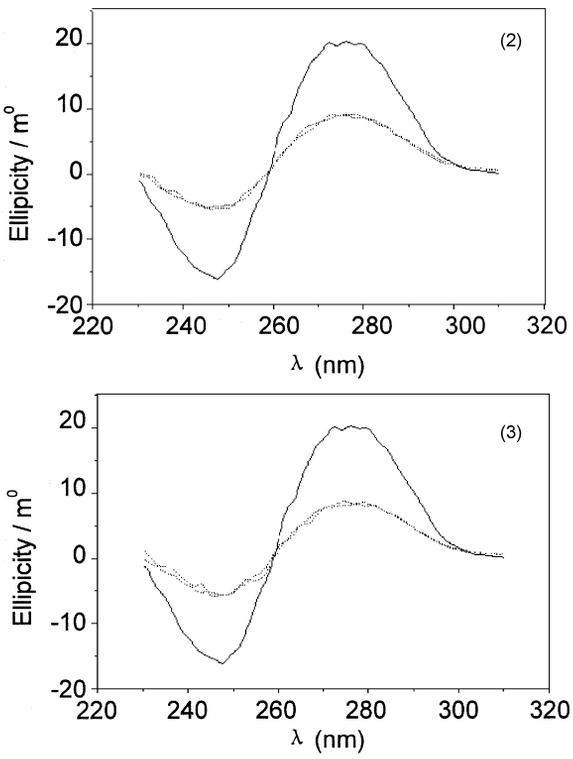

Fig. 4 CD spectra of DNA in the absence (—) and presence (- - -) of **2** and **3**. [DNA] = 1.0 mM.

complexes resulted in a decrease in the molecular ellipticity values of both the positive and negative ellipticity bands. As for **2** and **3**, the intensity of the negative ellipticity band decreases almost same to that for the positive ellipticity band. This suggests that the DNA-binding of the complexes do not affect the conformational changes of DNA.

Viscosity measurements

As a means of further clarifying the binding of the present copper complexes to DNA, viscosity measurements were carried out on CT DNA by varying the concentration of the added complexes. Spectroscopic data are necessary, but not sufficient to support a binding mode. In the absence of crystallographic structure data, hydrodynamic measurements, which are sensitive to DNA length increases, are regarded as the least ambiguous and the most critical tests of binding in solution.[34] A classical intercalative mode causes a significant increase in viscosity of the DNA solution due to an increase in the separation of base pairs at the intercalation sites and hence an increase in overall DNA length. In contrast, groove-face or electrostatic interactions typically cause less pronounced (positive or negative) or no change in the DNA solution viscosity.[26] A partial or nonclassical intercalation of the ligand would reduce the DNA viscosity.[35] Values of $(\eta/\eta_0)^{1/3}$ were plotted against $[CuL]^{2+}$/[DNA] in the absence and presence of the copper complexes (Fig. 5). The presence of complexes **1** and **3** had no obvious effect on the viscosity of CT DNA whereas that of complex **2** slightly decreases the relative viscosity of the DNA solution. Considering the insignificant hyperchromism and red shift of **1** and **3** by the addition of DNA, it is suggested that the electrostatic interaction of the complexes with DNA may be the main binding pattern. As for **2**, the decreased relative viscosity of DNA may be explained by a binding mode

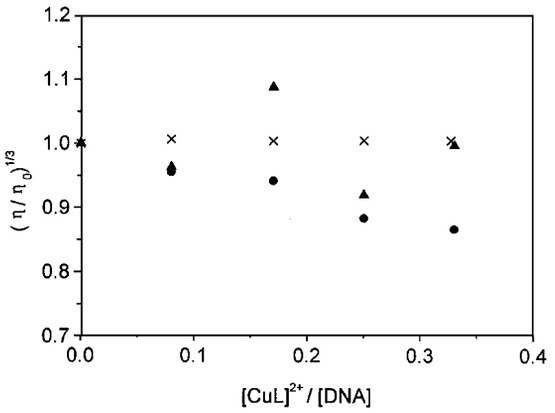

Fig. 5 Effects of increasing amounts of **1** (▲), **2** (●) and **3** (×) on the relative viscosities of CT DNA

which produced bends or kinks in the DNA and thus reduced its effective length and concomitantly its viscosity. The results suggest that complex **2** may bind to DNA by partial intercalation. It is also implied that classical intercalation could be ruled out for **1** and **3**.

Cleavage of pUC18 DNA

The characterization of DNA recognition by transition metal complexes has been aided by the DNA cleavage chemistry that is associated with redox-active or photoactivated metal complexes. The consequence of DNA cleavage is relaxation of the supercoiled circular form of pUC18 DNA into a nicked circular form and linear form. When circular plasmid DNA is subjected to electrophoresis, the fasterest migration will be observed for the supercoiled form (Form I). If one strand is cleaved, the supercoiled form will relax to produce a slower-moving open circular form (Form II). If both strands are cleaved, a linear form (Form III) will be generated that migrates in between.

Fig. 6 illustrates the gel electrophoretic separations showing the cleavage of plasmid pUC18 DNA induced by the three complexes under identical reaction conditions using 2-mercaptoethanol and/or H_2O_2 activation, respectively. As shown in Fig. 6, only in the presence of H_2O_2 and 2-mercaptoethanol can the complexes **1**, **2** and **3** convert supercoiled plasmid pUC18 DNA to a mixture of supercoiled (Form I) and nicked (Form II) DNA. Activated by 2-mercaptoethanol without H_2O_2 or activated by H_2O_2 without 2-mercaptoethanol, the complexes are incapable of cleaving plasmid DNA. It can be seen that neither the copper(II) complexes nor incubation with H_2O_2 or 2-mercaptoethanol without the complexes yields DNA strand scission. It can also be seen that with increasing concentrations of H_2O_2 and 2-mercaptoethanol, Form II does not increase gradually [Fig. 6(B), lanes 5, 6]. It is likely that the generation of hydroxy radicals and/or activated oxygen mediated by the copper complexes results in DNA cleavage. Further studies are currently underway to clarify the cleavage mechanism.

Conclusions

By the incorporation of simple modifications on the side chains of tetraaza macrocyclic ligand, different DNA-binding behaviors of **1**, **2** and **3** have been suggested. Spectroscopic studies together with viscosity experiments support that complexes **1** and **3** may bind to DNA by electrostatic interaction. Complex **2** with an aromatic moiety group on the side chain binds to DNA more strongly than **1** and **3**, and whose interaction with DNA may be partial intercalation *via* the aromatic ring into the base pairs of DNA. The complexes exhibit effective nuclease activities upon activation of 2-mercaptoethanol and H_2O_2, resulting in the DNA cleavage from the double-

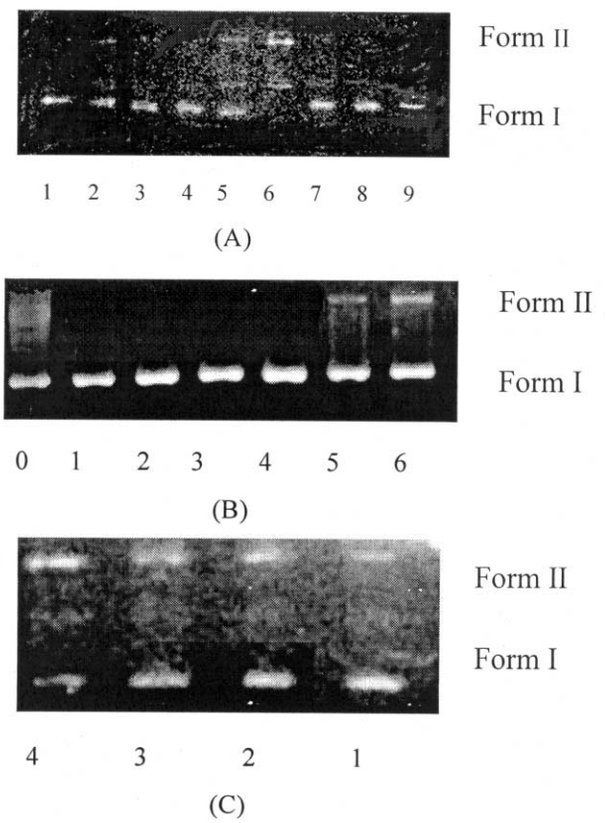

Fig. 6 Electrophoretic separations showing the cleavage of pUC18 DNA induced by **1** (A), **2** (B) and **3** (C). (A) DNA + $[CuL^1]^{2+}$ (lane 1); DNA + $[CuL^1]^{2+}$ + 2-mercaptoethanol (0.15 mM) (lane 2); DNA + $[CuL^1]^{2+}$ + 2-mercaptoethanol (0.30 mM) (lane 3); DNA + $[CuL^1]^{2+}$ + H_2O_2 (0.15 mM) (lane 4); DNA + $[CuL^1]^{2+}$ + H_2O_2 (0.30 mM) (lane 5); DNA + $[CuL^1]^{2+}$ + H_2O_2 (0.15 mM) + 2-mercaptoethanol (0.15 mM) (lane 6); DNA + H_2O_2 (0.15 mM) (lane 7); DNA + 2-mercaptoethanol (0.15 mM) (lane 8); DNA + H_2O_2 (0.15 mM) + 2-mercaptoethanol (0.15 mM) (lane 9). (B) DNA (lane 0); DNA + $[CuL^2]^{2+}$ (lane 1); DNA + $[CuL^2]^{2+}$ + H_2O_2 (0.15 mM) (lane 2); DNA + $[CuL^2]^{2+}$ + 2-mercaptoethanol (0.15 mM) (lane 3); DNA + H_2O_2 (0.15 mM) + 2-mercaptoethanol (0.15 mM) (lane 4); DNA + $[CuL^2]^{2+}$ + H_2O_2 (0.15 mM) + 2-mercaptoethanol (0.15 mM) (lane 5); DNA + $[CuL^2]^{2+}$ + H_2O_2 (0.30 mM) + 2-mercaptoethanol (0.30 mM) (lane 6). (C) DNA + $[CuL^3]^{2+}$ (lane 1); DNA + $[CuL^3]^{2+}$ + 2-mercaptoethanol (0.15 mM) (lane 2); DNA + $[CuL^3]^{2+}$ + H_2O_2 (0.15 mM) (lane 3); DNA + $[CuL^3]^{2+}$ + H_2O_2 (0.15 mM) + 2-mercaptoethanol (0.15 mM) (lane 4).

stranded to single-standed one. Thus, the present study suggests that the structure of the side chain attached to the macrocycle plays an important role in governing the nature of the binding with DNA. The existence of a planar ring on the side chain contributes to the intercalation of the complex into DNA.

Acknowledgements

We are grateful to the National Science Foundation of China, the Natural Science Foundation of Guangdong Province, the State Key Laboratory of Coordination Chemistry in Nanjing University, the State Key Laboratory of Bio-organic and Natural Products Chemistry in the Shanghai Institute of Organic Chemistry and the Research Fund of the Royal Society of Chemistry, UK, for their financial support.

References

1 C. J. Burrows and S. E. Rokita, *Acc. Chem. Res.*, 1994, **27**, 295.
2 X. Y. Chen, S. E. Rokita and C. J. Burrows, *J. Am. Chem. Soc.*, 1991, **113**, 5884.
3 C. J. Burrows and J. G. Muller, *Chem. Rev.*, 1998, **98**, 1109.
4 H. C. Shih, N. Tang, C. J. Burrows and S. E. Rokita, *J. Am. Chem. Soc.*, 1998, **120**, 3284.
5 X. Y. Chen, C. J. Burrows and S. E. Rokita, *J. Am. Chem. Soc.*, 1992, **114**, 322.
6 J. G. Muller, P. Zheng, S. E. Rokita and C. J. Burrows, *J. Am. Chem. Soc.*, 1996, **118**, 2320.
7 R. P. Hickerson, R. J. Perez and C. J. Burrows, *J. Am. Chem. Soc.*, 1997, **119**, 1501.
8 J. P. Sluka, S. J. Horvath, M. F. Bruist and P. B. Dervan, *Science*, 1987, **238**, 1129.
9 C. L. Liu, J. Y. Zhou, Q. X. Li, L. J. Wang, Z. R. Liao and H. B. Xu, *J. Inorg. Biochem.*, 1999, **75**, 233.
10 M. Shionoyan and E. Kimura, *Chemistry*, 1992, **47**, 878.
11 C. L. Liu, J. Y. Zhou, Q. X. Li, L. J. Wang, Z. R. Liao and H. B. Xu, *Inorg. Chem. Acta*, 1998, **3**, 253 (in Chinese).
12 C. L. Liu, J. Y. Zhou and H. B. Xu, *J. Inorg. Biochem.*, 1998, **71**, 1.
13 D. K. Chand, H. J. Schneider, J. A. Aguilar, F. Escarti, E. Garcia-Esspara and S. V. Luis, *Inorg. Chim. Acta*, 2001, **316**, 71.
14 D. Y. Kong, A. E. Martell and R. J. Motekaitis, *J. Inorg. Biochem.*, 2001, **86**, 298.
15 J. Liu, T. X. Zhang, T. B. Lu, L. H. Qu, H. Zhou, Q. L. Zhang and L. N. Ji, *J. Inorg. Biochem.*, 2002, **91**, 269.
16 J. Liu and L. N. Ji, *Acta Sci. Nat. Univ. Sunyatseni*, 2001, **40**, 121.
17 J. Marmur, *J. Mol. Biol.*, 1961, **3**, 208.
18 M. E. Reichmann, S. A. Rice, C. A. Thomas and P. Doty, *J. Am. Chem. Soc.*, 1954, **76**, 3047.
19 J. B. Chaires, N. Dattagupta and D. M. Crothers, *Biochemistry*, 1982, **21**, 3933.
20 S. Satyanarayana, J. C. Daborusak and J. B. Chaires, *Biochemistry*, 1993, **32**, 2573.
21 G. M. Sheldrick, SHELXL-93, Program for X-Ray Crystal Structure Refinement, University of Göttingen, Germany, 1993.
22 L. Ballester, A. M. Gil, A. Gutierrez and M. F. Perpinan, *Inorg. Chem.*, 2000, **39**, 2837.
23 M. T. Azcondo, L. Ballester, A. Gutierrez, M. F. Perpinan, U. Amador, C. Ruiz-Valero and C. Bellitto, *J. Chem. Soc., Dalton Trans.*, 1996, 3015.
24 M. P. Suh, B. Y. Shim and T. S. Yoon, *Inorg. Chem.*, 1994, **33**, 5509.
25 S. A. Tysoe, R. J. Morgan, A. D. Baker and T. C. Strekas, *J. Phys. Chem.*, 1993, **97**, 1707.
26 T. M. Kelly, A. B. Tossi, D. J. McConnell and T. C. Strekas, *Nucleic Acids Res.*, 1985, **13**, 6017.
27 M. Sethuraman and P. Mallayan, *Inorg. Chem.*, 1998, **37**, 693.
28 L. A. Lipscomb, F. X. Zhou, S. R. Presnell, R. J. Woo, M. E. Peek, R. R. Plaskon and L. D. Williams, *Biochemistry*, 1996, **35**, 2818.
29 R. F. Pasternack, E. J. Gibbs and J. J. Villafranca, *Biochemistry*, 1983, **22**, 2406.
30 A. Wolfe, G. H. Shimer and T. Meehan, *Biochemistry*, 1987, **26**, 6392.
31 J. B. LePecq and C. Paoletti, *J. Mol. Biol.*, 1967, **27**, 87.
32 B. C. Baguley and M. LeBret, *Biochemistry*, 1984, **23**, 937.
33 R. F. Pasternack, M. Cacca, B. Keogh, T. A. Stephenson, A. P. Williams and F. J. Gibbs, *J. Am. Chem. Soc.*, 1991, **113**, 6835.
34 S. Satyanarayana, J. C. Daborusak and J. B. Chaires, *Biochemistry*, 1992, **31**, 9319.
35 G. Yang, J. Z. Wu, L. Wang, L. N. Ji and X. Tian, *J. Inorg. Biochem.*, 1997, **66**, 141.